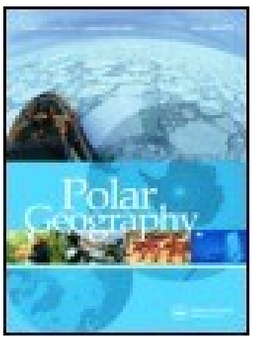

Polar Geography

ISSN: (Print) (Online) Journal homepage: https://www.tandfonline.com/loi/tpog20

Long-term Circumpolar Active Layer Monitoring (CALM) program observations in Northern Alaskan tundra

Kelsey E. Nyland, Nikolay I. Shiklomanov, Dmitry A. Streletskiy, Frederick E. Nelson, Anna E. Klene & Alexander L. Kholodov

To cite this article: Kelsey E. Nyland, Nikolay I. Shiklomanov, Dmitry A. Streletskiy, Frederick E. Nelson, Anna E. Klene & Alexander L. Kholodov (2021): Long-term Circumpolar Active Layer Monitoring (CALM) program observations in Northern Alaskan tundra, Polar Geography, DOI: 10.1080/1088937X.2021.1988000

To link to this article: https://doi.org/10.1080/1088937X.2021.1988000

Published online: 14 Oct 2021.

POLAR GEOGRAPHY
https://doi.org/10.1080/1088937X.2021.1988000

Taylor & Francis
Taylor & Francis Group

Long-term Circumpolar Active Layer Monitoring (CALM) program observations in Northern Alaskan tundra

Kelsey E. Nyland [a], Nikolay I. Shiklomanov [a], Dmitry A. Streletskiy [a], Frederick E. Nelson [b,c], Anna E. Klene [d] and Alexander L. Kholodov [e]

[a]Geography Department, George Washington University, Washington, DC, USA; [b]Department of Earth, Environmental and Geographical Sciences, Northern Michigan University, Marquette, MI, USA; [c]Department of Geography, Environment, and Spatial Sciences, Michigan State University, East Lansing, MI, USA; [d]Department of Geography, W.A. Franke College of Forestry and Conservation, University of Montana, Missoula, MT, USA; [e]Geophysical Institute, University of Alaska Fairbanks, Fairbanks, AK, USA

ABSTRACT

The Circumpolar Active Layer Monitoring (CALM) network is an ongoing international effort to collect and disseminate standardized measurements of active-layer dynamics to monitor the response of near-surface permafrost parameters to climate change. This work presents a distillation of 25 years (1995–2019) of observations from three north–south transects of CALM sites in tundra environments of Alaska. Transects examined in this work bisect tundra regions of discontinuous permafrost on the Seward Peninsula, and the continuous permafrost zone on the western and eastern sections of the Arctic Foothills and Arctic Coastal Plain. These transects represent regional climatic gradients, several physiographic provinces, and regionally characteristic landcover associations. Total active-layer thickening at observed sites ranged from 7 to 26 cm; more significant thaw occurred in the foothills despite less pronounced warming air temperature trends. This summary highlights several regional active layer responses to climate warming, complicated by distinct thermal landscape sensitivities, landscape variability, and documented thaw subsidence. Data summarized in this report are publicly available and represent an important validation resource for earth-system models that include regions in the continuous and discontinuous permafrost zones of northern and western Alaska.

ARTICLE HISTORY
Received 30 November 2020
Accepted 28 September 2021

KEYWORDS
Circumpolar Active Layer Monitoring; active layer; permafrost; monitoring; climate change; Alaska

Introduction

The term *active layer* refers to the layer of earth materials between the ground surface and the top of permafrost (perennially frozen ground) that thaws annually. This dynamic freeze/thaw cycling makes the active layer of particular importance to a wide variety of geomorphologic, hydrologic, ecological, and anthropogenic systems and processes across permafrost regions which occupy nearly a quarter of the Earth's land surface (Zhang et al., 2008). Given the current rapid Arctic climate warming, active-layer thickness (ALT) has been observed increasing in many regions (e.g. Abramov et al., 2019; Strand et al., 2021; Vasiliev et al., 2020). Increasing ALT can induce thermokarst processes, promote the

CONTACT Kelsey E. Nyland knyland@gwu.edu

proliferation of woody plant species, and enhance microbial activity and decomposition processes that release greenhouse gasses into the atmosphere (e.g. IPCC, 2019).

The Circumpolar Active Layer Monitoring (CALM) program was founded in the early 1990s. One of CALM's initial functions was to operate as a data-rescue program following the dissolution of the Soviet Union. In its initial phases CALM focused on preserving records of ALT from the territory of the USSR and North America. Records from Alaska were surprisingly few and, with few exceptions, were of relatively short duration and had been collected primarily in support of ecological, hydrological, and engineering investigations. An important concomitant goal of the fledgling CALM program in Alaska was to extend the few existing records and to establish new long-term monitoring sites that could serve the variety of original study purposes. Several of these sites were used to develop and test field procedures, sampling designs, data-analysis procedures, and data management. The Alaska component of the CALM program has been funded continuously by the U.S. National Science Foundation (NSF) since 1998. A short history of the CALM program forms the introduction to this special issue of *Polar Geography*.

Presented here is a summary of climatic and active layer observations and discussion of the reaction of the near-surface permafrost system to regional climate variation at the 24 Alaskan CALM tundra sites with a minimum of 10 consecutive years of direct ALT measurements and sufficient on-site meteorological data for climate analysis. Sites examined in this work are arranged into three north–south transects representative of (1) varying degrees of continentality; (2) several different physiographic provinces; and (3) representative landcover types. Trends exhibited at these different spatial scales provide the basis for a discussion about observed regional active-layer dynamics in response to climate variability under different landscapes across northern and western Alaska. The data description and analyses provided here illustrate fulfillment of the ongoing objectives of the CALM program:

(1) Maintain established programs of long-term active layer, near-surface permafrost, landscape, and geomorphic observations in existing regional networks;
(2) Expand CALM observational networks to representative cold-region sites with strategic emphasis on currently unrepresented regions and on co-location with sites in the Thermal State of Permafrost (TSP) borehole network;
(3) Continue development and refinement of data management and archiving activities and strategies, and provide data management and archiving support.

Study area and data

The Alaskan component of the CALM program consists of a total of 67 sites either directly supported by NSF or providing data on a volunteer basis. Of the currently active sites (those that have data reported within the last three years, i.e. since 2017), 24 offer long-term records (>10 consecutive years of reported data) that employ direct ALT measurement methods in tundra landscapes (Figure 1). The different sampling strategies employed at these sites are elaborated on in the following section. Using the international CALM site code provided in Figure 1 inset maps and in the following descriptions of site transects, additional metadata, including local place names, site photos, and detailed site descriptions, can be found online at the CALM website (www2.gwu.edu/~calm), the Global Terrestrial

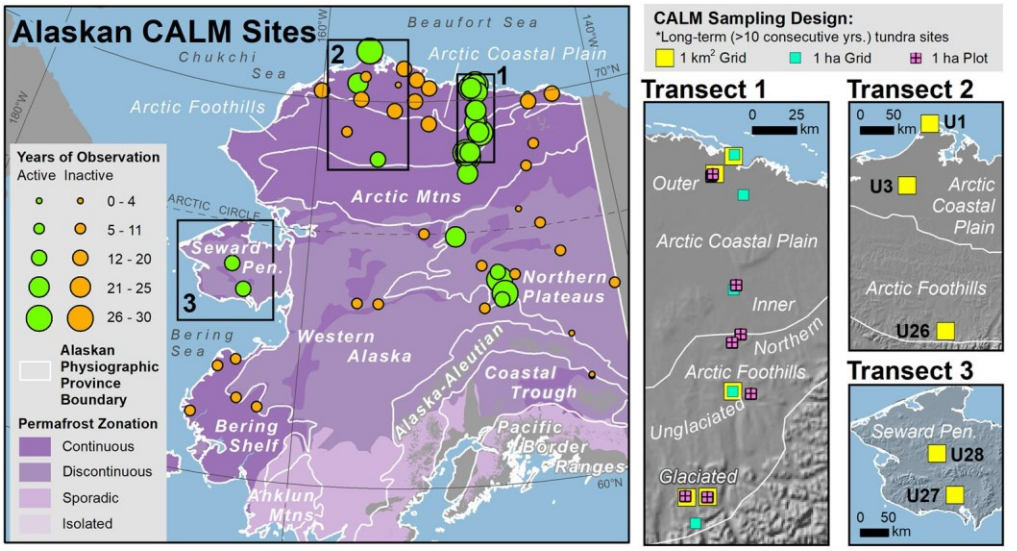

Figure 1. Alaskan CALM site locations, physiographic provinces (Wahrhaftig, 1965), and permafrost zones (Brown et al., 2002). Graduated symbols indicate length of observation records. Active sites have data available from within the last three years (since 2017). Inset maps show site sampling designs included in this report. Sites are labeled with international CALM site codes. Transect 1 sites are grouped by physiographic subregions: Outer Coastal Plain (sites U4, U5 and U6 U7A/B/C), Inner Coastal Plain (U8 and U31), Northern Arctic Foothills (U32A/B), Unglaciated Arctic Foothills (U9A/B and U10), and Glaciated Arctic Foothills (U11A/B/C, U12A/B, and U14).

Network for Permafrost database (gtnp.arcticportal.org), or the Arctic Data Center (arcticdata.io). Sites form roughly north–south transects spanning the eastern North Slope (area north of the Brooks Range) (Transect 1), the western North Slope (Transect 2), and the Seward Peninsula (Transect 3). From west to east these transects represent increasingly continental climatic conditions.

Transects 1 and 2 are entirely within the zone of continuous permafrost on the North Slope (Brown et al., 2002). Both Transects 1 and 2 intersect tundra and subpolar climates, or ET and Dfc according to the Köppen-Geiger climate classification system, respectively (Peel et al., 2007).

Transect 1 has the greatest density of sites and variety of observations, including on-site thermal and subsidence monitoring, in addition to ALT. Most of the 19 sites in Transect 1 were established by the CALM and TSP programs or adopted from NSF Arctic System Science (ARCSS) projects. Two of the 1 km² grid sites (U12A, at Toolik Lake, and U11A, at Imnavait Creek) were established under the U.S. Department of Energy's Response, Resistance, Resilience, and Recovery (R4D) program in the late 1980s (Hinzman et al., 1991; Kane et al., 1991; Walker et al., 1989). The 1 ha plots were originally part of the Arctic Flux Study within the larger ARCSS program, established to monitor trace gas release in tundra environments (Kane & Reeburgh, 1998; Klene et al., 2001; Nelson et al., 1997; Weller et al., 1995).

Physiographic sub-regions covered by Transect 1 include, from north to south, the Outer Arctic Coastal Plain (sites U4, U5, U6, and U7A/B/C), the Inner Arctic Coastal Plain (sites U8 and U56), the northern Arctic Foothills (sites U32A/B), the unglaciated southern Arctic

Foothills (sites U9A/B, U10), and the glaciated southern Arctic Foothills (sites U11A/B/C, U12A/B, U14). The Arctic Coastal Plain has low relief, with localized polygonal uplands and thermokarst features with poor drainage. The outer Arctic Coastal Plain has ubiquitous ponds and lakes, while the inner Arctic Coastal Plain has fewer lakes due to the gradual southward elevation increase toward its junction with the Arctic Foothills. The Arctic Foothills province has significantly more relief and better-developed drainage than the Arctic Coastal Plain, with hills and ridges throughout. The Arctic Foothills physiographic province was subdivided based on glacial history and relative elevation as it grades between the Arctic Coastal Plain to the north and Brooks Range to the south. Many of these sites were described in detail in an appendix to Brown et al. (2000).

Transect 2 extends from site U1 at Utqiaġvik (village formerly known as Barrow; the site name Barrow is retained here for record consistency) at the confluence of the Chukchi and Beaufort Seas on the Arctic Coastal Plain, south to the village of Atqasuk (U3), also on the Arctic Coastal Plain, then to the base of the Ivotuk Hills within the glaciated Arctic Foothills (U26). The 1 km^2 grids at sites U1 and U3 were originally established by the ARCSS program after extensive study in the vicinity of the sites by the Tundra Biome Program in the early 1970s (Brown et al., 1980). U1 is located on reworked marine silt deposits of the outer Arctic Coastal Plain (Hinkel & Nelson, 2003) and U3 is on the west bank of the Meade River on an ancient sand sea of the inner Arctic Coastal Plain (Carter, 1981; Everett, 1980). Site U26, originally established by the NSF-funded Arctic Transitions in the Land-Atmosphere System (ATLAS) project (McGuire et al., 2003), occupies terraces of Otuk Creek and contains several water tracks.

The two sites making up the westernmost transect (Transect 3) are former ATLAS sites in glaciated terrain of the southern Seward Peninsula. Landcover at these sites consists of tussock tundra interspersed with dense, tall shrubs (2–4 m in height). Site U28 is located near the Kougarok River on a south-facing slope in discontinuous permafrost (Brown et al., 2002) and site U27, near the village of Council, is on a relatively flat area underlain by sporadic permafrost (Brown et al., 2002). The entire Seward Peninsula physiographic province is classified as having a subpolar climate, or Dfc climate type (Peel et al., 2007). Dfc climates experience mean monthly air temperatures above 10°C for one to three months of the year and little seasonal differences in precipitation.

Data collection and analytical methods

Active-layer monitoring

The standard CALM protocol for direct measurement of ALT by mechanical probing is performed at all sites examined in this report. A metal rod, calibrated in cm, is inserted into the thawed ground to the point of refusal, interpreted in most instances as the frost table (yields measurements with 2 cm accuracy and ±0.5 cm precision) (Mackay, 1977). It is important to note that the date of maximum annual thaw can vary from year to year and between sites, making it difficult to detect the precise maximum annual active-layer thickness by mechanical probing. To ensure relative consistency throughout records, site-specific measurements are performed within the same Julian calendar week at least once a year within the maximum thaw season (mid-August to mid-September) (Brown et al., 2000; Hinkel & Nelson, 2003; Shiklomanov et al., 2008, 2012). Measurements at all sites included in this work are performed before August 31st of each year. Some sites have additional years of

data before 1995 excluded from subsequent analyses because measurement dates were outside the season of maximum thaw.

Sites included in this study feature one of three spatial sampling designs: 1 km² and 1 ha grids, and 1 ha plots. The 1 km² grids encompass generalized conditions and multiple landforms characteristic of a given physiographic province. The 1 ha grids and plots are situated in homogenous vegetation and soil associations. Within the ten 1 km² grids (U1, U3, U5, U7A, U9B, U11A, U12A, U26, U27, and U28) the average of two measurements taken by mechanical probing are recorded over a grid of fixed, regularly spaced point locations at 100 m intervals and 10 m intervals for the five 1 ha grids (U4, U6, U8, U9A, and U14). This systematic sampling design yields a total of 121 recorded measurements used to calculate the annual average ALT for each site.

The gridded (systematic) sampling design was tested against several other sampling designs during the initial (pre-1995) stage of the CALM program and was found to accurately capture population mean and frequency-distribution characteristics while remaining logistically feasible and time efficient (Fagan & Nelson, 2017). Gridded arrays of evenly spaced fixed-point locations have become the most common CALM sampling design used in Alaska and Russia to monitor broad-scale ecological change (Brown et al., 2000; Hinkel & Nelson, 2003; Shiklomanov et al., 2008, 2012). Spatial autocorrelation, scales of variability, and spatial patterns of ALT on the 1 km² grids were addressed in a series of papers published in the early stages of the CALM program (Hinkel & Nelson, 2003; Nelson et al., 1997, 1998a, 1999).

The 1 ha plots were established in homogenous landcover categories specific to the Kuparuk River watershed identified by Auerbach et al. (1997). The units include wet tundra (Wet), moist nonacidic tundra (MNT), moist acidic tundra (MAT), and shrublands (Klene et al., 2001; Nelson et al., 1997; Nyland et al., 2012; Streletskiy et al., 2008). Vegetation, soils, and ALT data in these plots were used as the basis for regional mapping of ALT over a 26,278 km² area of the North Slope containing the Kuparuk River basin (Muller et al., 1998; Nelson et al., 1997; Shiklomanov & Nelson, 1999).

Examining areas of well-defined landcover units was previously found to be an effective indicator of subsurface conditions including soil types, soil acidity, and glaciation history (Walker et al., 1998). At the nine 1 ha plot sites in Transect 1 (U7B/C, U10, U11B/C, U12B, U56, U32A/B), ALT is measured by mechanical probing at 5 m intervals along two perpendicular and one diagonal transect. This transect-based sampling design, which was developed for Flux Study vegetation and soil surveys at each plot, yields 71 measurements and adequate spatial coverage. All 71 point measurements are used to calculate the annual average ALT at each plot.

Regional climate monitoring

To complement spatially oriented ALT measurements, all of the 1 ha plots and several of the 1 km² grids in Transect 1 are outfitted with thermal monitoring equipment. Temperature measurements were collected at one or two hour intervals, depending on the site, using Onset™ miniature temperature data loggers with thermistors installed in radiation shields at standard meteorological instrument height (1.6–2.0 m above the ground surface). The current generation of Onset™ miniature temperature data loggers (HOBO Pro v2) has an effective range from −50°C to +30°C with ± 0.2°C accuracy and 0.02°C precision at freezing (Onset Computer Corporation, Pocasset, Massachusetts). Three

generations of Onset loggers have been used at the sites; each time a new generation was introduced the new loggers and a subset of their predecessors were operated simultaneously at each site for at least one year to ensure continuity in measurement accuracy.

Climate records and edaphic information from geographically proximal or similar meteorological station locations were used for sites without CALM air temperature monitoring or to correlate with sites that have missing data in air temperature records. Additional climate databases utilized included those maintained by the Thermal State of Permafrost (TSP), the International Tundra Experiment (ITEX), the Water and Environmental Research Center (WERC), the US Department of Agriculture Natural Resources Conservation Service (NRCS), and the National Oceanic and Atmospheric Administration's National Centers for Environmental Information (NCEI). All records were standardized to daily mean values for each site, from which mean annual air temperature (MAAT) and degree days of thawing (DDT) were calculated. ALT and MAAT anomalies were calculated relative to the 10 year average of the 2006–2015 observation period. Degree Days of Thawing (DDT) were estimated by summing mean daily temperatures above 0°C until the particular date of measurement for each site (Klene et al., 2001; Shiklomanov & Nelson, 2003).

Subsidence monitoring

Beginning in 2001, frost heave and thaw subsidence observations were made in addition to ALT and air temperature measurements at sites U1 (Barrow 1 km^2 grid on the outer coastal plain in Transect 2), U5 (West Dock 1 km^2 grid on the outer coastal plan in Transect 1) and U32A (Sagwon Hills 1 ha plot in the northern foothills in Transect 1). The ground surface position is measured by rapid static Differential Global Positioning System (DGPS) surveying. DGPS surveying was performed using Trimble 4700/5700/R7 receivers with Zephyr antennas (Trimble Navigation Ltd, Sunnyvale, California) mounted on permanently installed targets in a hierarchical nested arrangement within each site (Little et al., 2003). The systematic vertical accuracy is estimated to be less than 0.02 m and depend on the distances between sites and the base stations (Shiklomanov et al., 2013). Post-processing of DGPS measurements to determine absolute vertical positions of the ground surface was performed using Trimble Geomatics Office software.

Results

Regional active-layer trends

To assess regional active-layer trends only gridded 1 km^2 and 1 ha sites were considered. Figure 2 shows anomalies in mean annual ALT relative to a 10-year reference period from the middle of the record (2006–2015) and MAAT for 1 km^2 and 1 ha grid sites along the three long-term CALM transects for the 1995–2019 observation period. Due to the density of sites in Transect 1 annual anomalies were averaged for proximal sites defined by the physiographic sub-regions in Figure 1. Changes in ALT were evaluated by fitting linear regression models for sites with at least10 consecutive years of data available. Descriptive statistics for all individual sites and site groupings in Transect 1 are shown in Table 1, along with significance (p-values) associated with all linear trends.

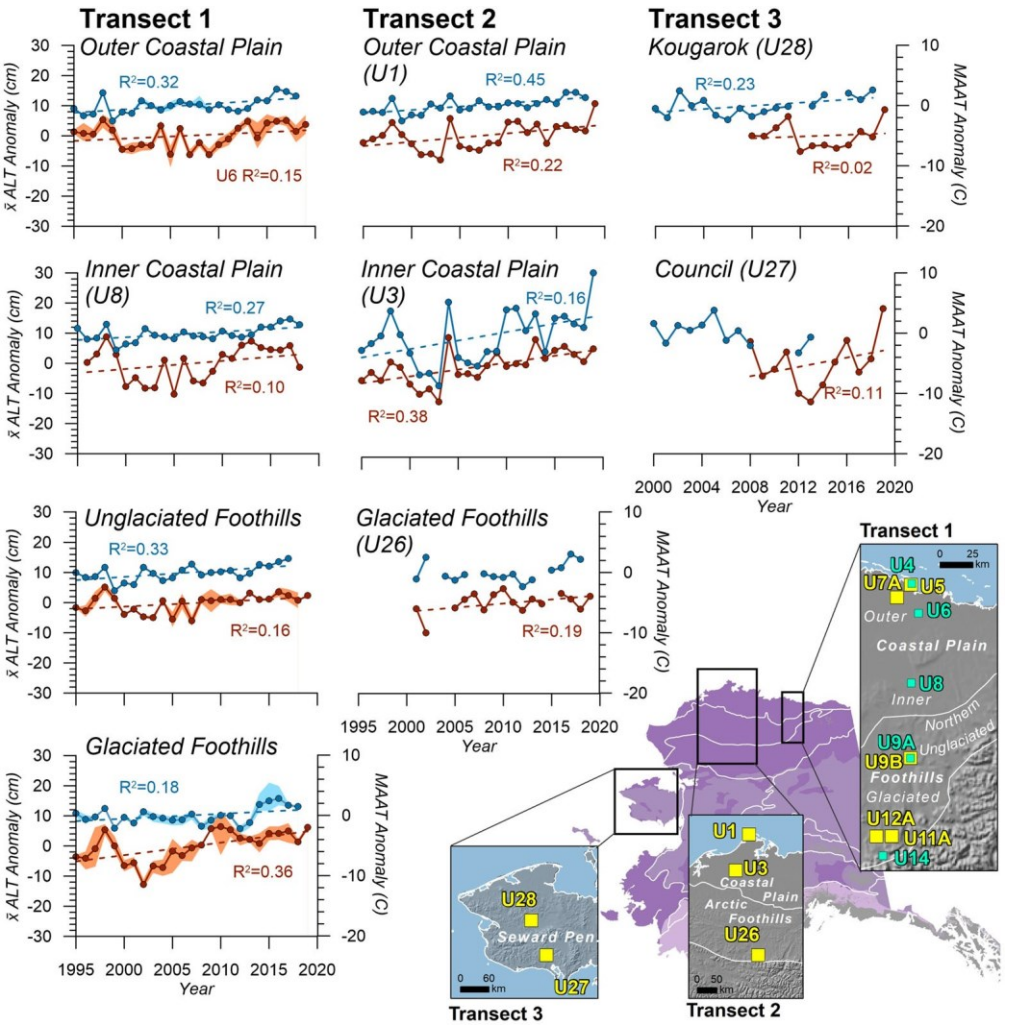

Figure 2. Three long-term, north-south, CALM transects. Graphs show anomalies in annual active layer thickness (ALT, orange lines, left y-axes) and mean annual air temperatures (MAAT, blue lines, right y-axes). Shaded areas show the range of values for grouped sites (refer to inset map). Dashed linear regression trend lines and associated R^2 values were generated in Grapher 10 Software for records from gridded sites with >10 years of consecutive data.

All regional groups of sites in Transect 1 show increasing MAAT trends. Rates of air temperature increase range from 0.07°C to 0.11°C/yr along this transect. Increasing trends in ALT for sites in these grouping, however, are much more variable. Generally higher and more statistically significant increasing ALT trends of 0.42–0.54 cm/yr were observed at sites in the southernmost glaciated Arctic Foothills in Transect 1, despite less warming observed there (0.07°C/yr).

Climate data from the coastal plain on Transect 2 (U1 and U3) show generally increasing MAAT over the 25 years (1995–2019) (Figure 2). However, the MAAT linear trend of 0.11°C/yr at site U1 displays greater significance (Table 1). The discontinuous air temperature records available near U26 precludes definitive long-term trend analysis. Similar to the

Table 1. Summary statistics for individual site records. Figure 3 inset map shows locations of sites in Transect 3 regional groups.

Geographic Name	Observation Type	Data Source	Site	*n*	Min.	*x*	Max.	σ	Trend
Transect 1									
Prudhoe Bay	MAAT	CALM/NRCS	U5 U7B/C	24	−13.02	−10.43	−7.54	1.39	0.11***
(Outer Coastal	ALT	CALM	U4	23	24.71	31.49	37.27	3.58	0.83**
Plain)	ALT	CALM	U5	25	43.94	50.72	57.70	4.23	0.11
	ALT	CALM	U6	22	55.50	65.70	72.81	5.18	0.31*
	ALT	CALM	U7A	25	46.27	52.71	59.73	3.89	0.01
			Regional ALT x	25	42.61	50.16	56.88	6.99	0.36*
Franklin Bluffs	MAAT	CALM/TSP	U8 U31	24	−12.96	−10.22	−7.81	1.25	0.09***
(Inner Coastal Plain)	ALT	CALM	U8	23	52.82	63.05	71.85	5.68	0.27
Happy Valley	MAAT	CALM/TSP	U9A/B	23	−12.75	−9.82	−7.45	1.27	0.11***
(Unglaciated	ALT	CALM	U9A	19	32.91	40.83	47.18	4.21	1.03**
Foothills)	ALT	CALM	U9B	25	39.56	44.32	48.75	2.76	0.09
			Regional ALT x	25	36.24	42.58	47.97	8.65	0.47**
Upper Kuparuk Watershed	MAAT	CALM/NRCS	U11B U12B U14	24	−9.81	−7.56	−5.70	1.12	0.07**
(Glaciated	ALT	CALM	U11A	25	38.81	52.22	62.89	6.04	0.54***
Foothills)	ALT	CALM	U12A	25	38.27	49.45	60.99	5.53	0.43***
	ALT	CALM	U14	20	39.00	52.85	60.00	5.60	0.20
			Regional ALT x	25	38.69	51.51	61.29	5.08	0.42**
Transect 2									
Utqiaġvik/Barrow	MAAT	NCEI	U1	24	−12.73	−10.15	−7.99	1.21	0.11***
(Outer Coastal Plain)	ALT	CALM		25	28.61	36.66	47.32	4.46	0.28**
Atqasuk	MAAT	NRCS/ITEX	U3	22	−12.28	−9.71	−6.99	1.43	0.09*
(Inner Coastal Plain)	ALT	CALM		25	37.38	49.04	58.73	5.47	0.46***
Ivotuk	MAAT	ATLAS/TSP/ NCEI	*<10 consecutive years of data*						
(Glaciated Foothills)	ALT	CALM	U26	16	42.75	52.61	57.38	3.45	0.27*
Transect 3									
Kougarok	MAAT (C)	ATLAS/NCEI		17	−5.90	−3.51	−0.91	1.57	0.13
	ALT (cm)	CALM	U28	12	56.19	61.43	70.14	4.26	0.15
Council	MAAT	TSP	*<10 consecutive years of data*						
	ALT	CALM	U27	12	54.52	67.24	85.46	8.53	0.77

Note: *$p<0.1$; **$p<0.05$; ***$p<0.01$

increasing MAAT trends, ALT at all three sites is also generally increasing. The greatest ALT trend was observed at U3, despite less pronounced warming compared to U1. This is likely due to differences in edaphic conditions. Site U3 is underlain by a large, well-drained sand deposit that promotes thaw and greater response to the climatic signal compared to U1 within polygonal peatland.

MAAT at Kougarok Creek displays an increasing linear trend of 0.13°C/yr. The relatively short air temperature record available for Council precludes any definitive analysis of long-term trends. ALT records for both sites do not show significant change over the period from 2008 to 2019. However, both sites show marked increases in thaw propagation since 2012. The warmest year (2019) resulted in the maximum ALT recorded at both sites, with 85.5 cm at U28, and 70.1 cm at U27. In the Garfield Creek fire in July of 2019 (Hovey, 2019), 54 out of the total 121 grid nodes (45%) within the site array were burned, likely contributing to the increase in thaw propagation.

Landscape-specific active-layer trends

The 1 ha plots within Transect 1 were selected to be representative of a variety of surface and subsurface conditions representative of the Kuparuk Basin (Nelson et al., 1997, p. 370). ALT trends from these 1 ha plots allow for a more detailed analysis of edaphic effects, specifically landcover and soil thermal properties, in relation to the square root of accumulated seasonal degree-days of thaw based variations of the Stefan Solution (e.g. Brown et al., 2000, p. 176; Nelson & Outcalt, 1987). Figure 3 shows the relations between ALT and DDT temporally and with $DDT^{1/2}$.

Similar to the temporal trends observed from gridded sites in the previous section, the more pronounced ALT increases observed in the 1 ha plots are apparent in the southern portions of Transect 1 despite a lack of distinct warming trends at these sites. Moving progressively south, the degree of ALT variability explained solely by climate forcing ($DDT^{1/2}$) decreases drastically, suggesting greater influences exerted by non-climatic, or edaphic, factors. As shown in Figure 3, in moist non-acidic tundra, summer climatic variability ($DDT^{1/2}$) accounts for 50% of ALT variability on the outer Coastal Plain (U7B) and 30%

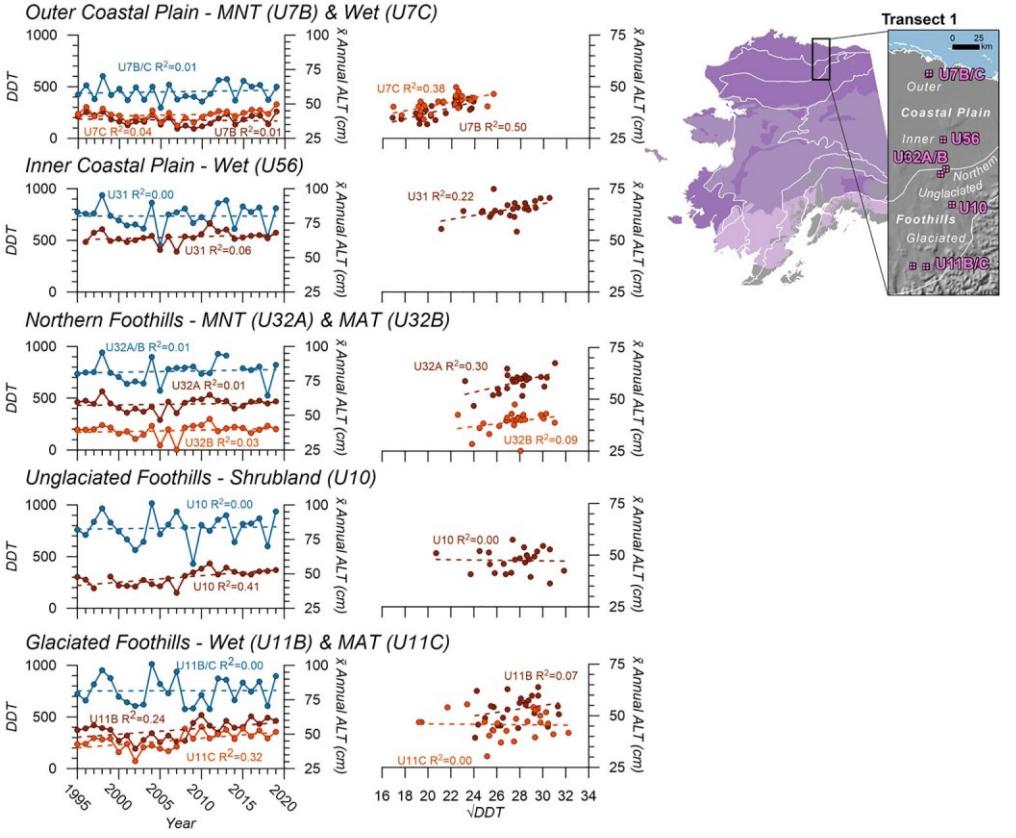

Figure 3. 1 ha plot records are arranged geographically where proximal sites are shown on the same graph and by location from north to south (top to bottom). The left column of graphs show annual degree days of thaw (DDT) (blue) and mean annual active layer thickness (ALT) (orange shades). The right column are correlations between mean annual ALT and $DDT^{1/2}$. All dashed lines are linear regression trend lines.

in the northern Foothills (U32A). In wet tundra, 38% of the variability observed is explained by climate on the outer Coastal Plain (U7C), 22% on the inner Coastal Plain (U56), and just 7% in the glaciated Foothills (U11B). In moist acidic tundra climate forcing accounts for just 9% of observed ALT variability in the northern Foothills (U32B) and 0% in the glaciated Foothills (U11C). Similarly, in shrubland (U10) none of the observed ALT variability could be explained solely by summer climate forcing.

Ground surface displacement

Compared to previous reports that examined the correspondence between ALT and annual DDT (Shiklomanov, 2001; Streletskiy et al., 2008), these sites, now with 25-year records, exhibit still weaker correspondences between ALT and climate. This weaker correspondence can be attributed to the transient layer thaw and thaw consolidation at the decadal scale (Shiklomanov et al., 2013). Thaw consolidation due to thaw penetration into the ice-rich transient layer at the boundary between the active layer and the permafrost table complicates ALT measurements obtained by mechanical probing. To correct for any frost heave or thaw subsidence at the ground surface, DGPS surveying was performed on the outer Arctic Coastal Plain at sites U1 near Utqiaġvik (formerly Barrow) and U5 near West Dock on the Prudhoe Bay Oilfield, and in the northern Arctic Foothills at site U32A near Sagwon. Figure 4 shows ALT measurements by mechanical probing corrected for changes in ground surface position relative to the ground surface elevation in 2000. Positive change is indicative of frost heave and negative change is indicative of subsidence related to thaw consolidation. A net negative change, or subsidence, of 12 cm at sites U1 and U5, and 15 cm at site U32A was observed over the 18 years of observation.

Correlation graphs included in Figure 4 relating $DDT^{1/2}$ to both ALT, as measured from mechanical probing, and ALT adjusted for subsidence, suggest only limited influence of climate forcing, even when accounting for subsidence. While the relation between climate and ALT was strengthened after accounting for subsidence at site U1 the opposite impact was observed after correcting records from sites U5 and U32A. These results are similar to those from the 1 ha plots in Transect 1, suggesting greater influences of non-climatic, or edaphic, factors.

Discussion

Regional climate and active-layer trends

All three transects contained sites with records showing statistically significant increases in air temperature. This is reflective of the regional +1.8°C air temperature anomaly detected for the entire Alaskan North Slope and the Seward Peninsula over the 2000–2016 period relative to the 1981–2010 mean based on climate reanalysis (Romanovsky et al., 2020). In response to climate warming, mean annual ground temperatures on the Arctic Coastal Plain and Arctic Foothills have increased 0.42°C to 0.69°C and 0.33°C to 0.42°C per decade, respectively, as reported from TSP borehole records proximal to CALM sites for the 2000–2018 period (Romanovsky et al., 2020). Statistically significant increases in ALT were, however, detected only on the inner Arctic Coastal Plain in Transect 2 and in the southern glaciated Arctic Foothills in Transect 1 (Figure 2). Many ecosystem factors contribute to the regional and local heterogeneity, including the variable reaction of various

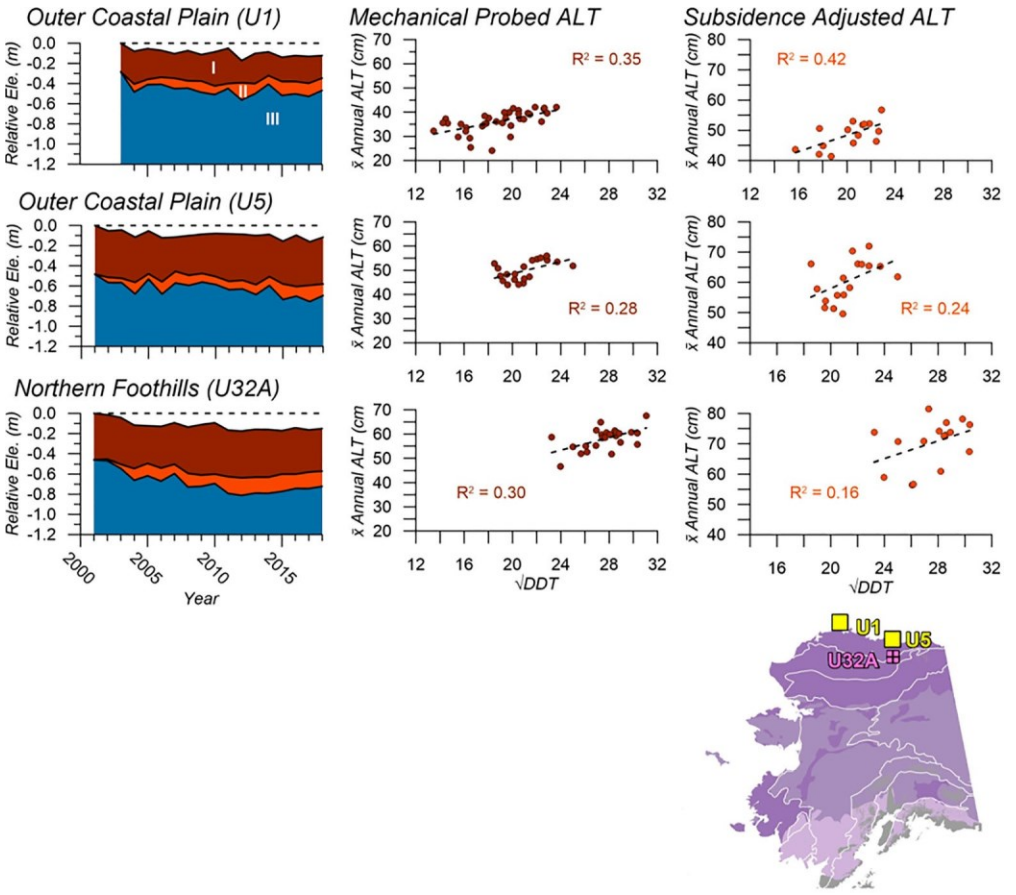

Figure 4. Annual change in ground surface position (left column graphs) on the Arctic Coastal Plain (U1 and U5) and Arctic Foothills (U32A). Shaded areas represent active layer thickness (ALT) as measured by mechanical probing (I), ALT corrected for ground subsidence (II), and permafrost (III). The datum position of the ground surface at the start of the measurement period is indicated by a dashed line. The middle column are correlations between mean annual ALT from mechanical probing and $DDT^{1/2}$. The right column are correlations between ALT adjusted for subsidence and DDT1/2. All dashed lines are linear regression trend lines.

landcover types to summer climate and isotropic, or regional, thaw subsidence. While the 1 km^2 grids provide generalized trends by encompassing multiple landscape units, more detailed and finer spatial scale measurements and analysis are required to assess the complex relations between climatic and non-climatic factors and ALT.

Climatic and edaphic influences on active-layer variability

Also contributing to the regional and local heterogeneity of ALT are landcover-specific thermal sensitivities. The decreased explanatory power of climate for observed ALT variability moving south along Transect 1 (Figure 3) indicates that landcover types with relatively taller deciduous shrub species modulate the warm air climate signal to the underlying ground during the summer season. The apparent disconnect between climate and ALT reaction can then be attributed to increasing variability of landscapes in the

Arctic Foothills, and particularly the relative abundance of taller woody species such as those found in moist acidic tundra (MAT) and shrublands (Shrub). Table 2 shows the greater variability in topography and landcovers within the 1 km² grid sites in Transect 1. Additionally, changes to and transitions between these landcover types can potentially represent shifts between negative to positive vegetation-permafrost feedback mechanisms (Shur & Jorgenson, 2007).

Remote sensing studies have indicated that widespread Arctic vegetation 'greening' and 'browning' are occurring in response to climatic change (e.g. Bhatt et al., 2017; Frost & Epstein, 2014; Raynolds & Walker, 2016). Both are supported by *in situ* studies that have documented significant increases in biomass accumulation at the ground surface (e.g. Elmendorf et al., 2012; Zamin et al., 2014), changes in water and disturbance regimes (Lara et al., 2018; Raynolds & Walker, 2016), spatial heterogeneity (Assmann et al., 2020; Lara et al., 2018) and the expansion and proliferation of deciduous shrubs (e.g. Forbes et al., 2010; Myers-Smith et al., 2011; Tape et al., 2006). Both positive and negative feedback mechanisms are associated with greening and browning trends that impose long-term (multi-decadal time scale) non-linear effects on the active layer and permafrost below. Increasing vegetation density and height can produce a positive feedback by warming the ground, causing permafrost degradation through reduced surface albedo and increased snow retention in winter (Ng & Miller, 1975; Sturm et al., 2001). Simultaneously, a proliferation of vegetation can also cool the ground, contributing to permafrost aggradation, through increased insulation and shading during the summer months (e.g. Domine et al., 2016; Lawrence & Swenson, 2011).

At present, the overall effect of landcover changes on permafrost is largely unquantified, resulting in significant uncertainties regarding any long-term responses of the permafrost system. While the initial results of long-term monitoring presented here point to complex relationships through simple regressions, a number of exogenous factors, including the insulation afforded by different vegetation communities and snow conditions, require further explicit investigation. The existence of feedback mechanisms impacting ALT and near-surface permafrost involves many ecosystem factors that can significantly affect the sensitivity of permafrost landscapes to climatic variability and change.

Transient layer thaw and ground surface subsidence

Relative ALT stability at sites not exhibiting significant change over the observation period, as shown in Figure 2, may also be partially explained by long-term subsidence as the active and transient layers are highly integrated components of the permafrost system

Table 2. Topographic and landcover characteristics of 1 km² grid sites in Transect 1.

		Landcover (% of 1 km²)				
1 km² Site	Elevation Range (masl)	MNT	MAT	Wet	Shrub	Water/Barren
Outer Coastal Plain (Prudhoe Bay)						
U7A	10–15	40.5	0.0	35.0	0.0	24.5
U5	2–5	37.0	0.0	36.0	0.0	27.0
Unglaciated Foothills (Happy Valley)						
U9B	295–342	18.0	26.5	0.5	54.0	1.5
Glaciated Foothills (Upper Kuparuk Watershed)						
U11A	875–941	19.0	48.0	2.0	31.0	0.0
U12A	715–775	21.0	43.0	0.5	26.5	9.0

(Shiklomanov et al., 2013; Shur et al., 2005; Streletskiy et al., 2017). Periodic ice aggradation and degradation within the transient layer at the interface between the active layer and permafrost can produce heave or thaw, respectively (Nelson et al., 2008; Shur et al., 2005). In ice-rich terrain such as sites U5 and U32A (Figure 4) the active layer appears to be relatively stable until measurements from mechanical probing are corrected for long-term, progressive thaw penetration and downward displacement of the ground surface (Shiklomanov et al., 2013; Streletskiy et al., 2017). This result indicates that entire natural landscapes underlain by ice-rich permafrost may be subsiding in response to climate warming. The relatively homogeneous, slow, geographically widespread, and low-magnitude subsidence observed is referred to as isotropic thaw subsidence, to distinguish it from the more localized, irregular, and relatively large-magnitude subsidence associated with thermokarst processes (Liu et al., 2010; 2012; Shiklomanov et al., 2013).

The active layer has also been shown to exhibit Markovian-like behavior (Nelson et al., 1998b, 2008; Streletskiy et al., 2017). An abnormally warm summer can cause frost penetration into the transient layer, resetting active-layer thickness (ALT) to a tightly constrained range about a new mean value over a consecutive series of ensuing years. Conversely, climatically extreme cool summers can reset ALT to lower values for subsequent years. The data sets used to test this hypothesis have been expanded substantially relative to those used in the studies cited above through use of long-term CALM records. Unlike the earlier studies, these include subsidence records in addition to the meteorological and ALT observations. As records from CALM sites have lengthened to multi-decadal series, departures from the standard bivariate Stefan relation between ALT and annual degree days of thaw have become more apparent (Streletskiy et al., 2017). The frequency of ALT 'resets', which may increase with climate variability, may account for the lack of correspondence observed considering the entire record on the correlation plots corrected for subsidence in Figure 4 (see plots for sites U5 and U32A). This topic is receiving high priority in the most recent iteration of funded work (CALM V) in Alaska (Nyland et al., 2020).

Conclusions

Collectively, the quarter-century of continuous, standardized observation records from the Alaskan CALM sites presented here constitute a brief summary of long-term active-layer dynamics in tundra landscapes characteristic of many Arctic regions. The greatest air temperature increases observed were at sites on the Arctic Coastal Plain where MAAT cumulatively increased by 2.75°C over the past 25 years (1995–2019). Significant changes in ALT over the same period, however, occurred at sites in the Arctic Foothills. Along Transect 2 (western North Slope), cumulative increases in mean annual ALT ranged from 7.00 to 11.5 cm, while thickening from 10.50 to 25.75 cm was detected at sites in Transect 1 (eastern North Slope) in the Arctic Foothills.

Northern Alaska is experiencing some of the lowest rates of ALT increase of any region represented in the CALM program (Romanovsky et al., 2020). Differences in landscape complexity and thaw subsidence only partially explain the relatively moderate trends and reduced response of ALT to regional summer warming trends. ALT measured by mechanical probing, corrected for thaw subsidence, also indicated long-term thaw propagation into the transient layer and ALT thickening not immediately apparent from mechanical probing records alone. However, even when subsidence is accounted for such as at sites U1, U5, and U32A, the relationship between ALT and degree days of thaw improves only slightly.

Additional edaphic factors require particular attention in light of the observed long-term discrepancies, particularly in more continental locations such as the Arctic Foothills where, although the climate is a primary driving factor for ALT, other factors increasingly modify these signals. These inland sites also require subsidence monitoring. Trends observed to date may be indicative of a transition from 'climate-driven' to 'climate-driven, ecosystem-modified' permafrost landscapes with continued warming and disturbance as outlined by Shur and Jorgenson (2007). Such a landscape functional transition underscores the importance of maintaining and expanding long-term, standardized CALM program site measurements. Ultimately, with significantly more data on subsidence and other edaphic factors at a wider variety of sites, landscape-based correction factors for ALT measurements from mechanical probing could be applied across the full data series.

Positive global climate feedbacks associated with permafrost change were recognized by the World Meterological Organization's (WMO) Global Climate Observing System (GCOS) when it identified permafrost temperature and active layer thickness (ALT) as essential climate variables (ECVs) (GCOS, 2003). The recognition of permafrost temperature and active-layer thickness as ECVs has fueled increasing numbers of permafrost modeling studies and applications. CALM data offer opportunities for model validation in a geographically comprehensive manner. Continuing and expanding on the CALM program objectives is therefore crucial for representing permafrost processes being incorporated into coupled general circulation (e.g. Fisher et al., 2018; Koven et al., 2013; Lawrence et al., 2012), hydrologic (e.g. Krogh et al., 2017), and ecosystem model (e.g. Chaudhary et al., 2017; Wania et al., 2009; Xia et al., 2017) projections of Arctic natural system responses to long-term climate change. Data for the entire CALM program are publically available through several public data platforms: the CALM website hosted by the George Washington University's Department of Geography, the NSF Arctic Data Center, and the Global Terrestrial Network for Permafrost (GTN-P).

Acknowledgements

The CALM network has been supported by U.S. National Science Foundation (NSF) awards OPP-9732051 to the University of Cincinnati, OPP-0352958 to the University of Delaware, and ARC-1002119, OPP-1304555, and OPP-1836377 to the George Washington University, and OPP-1836381 to Northern Michigan University and Michigan State University. Any opinions, findings, conclusions, or recommendations expressed in this work are those of the authors and do not necessarily reflect the views of the NSF. The mention of specific product names does not constitute an endorsement by the NSF. We are grateful to the numerous researchers and students who assisted in the field by conducting CALM observations and providing data. Dr. Jerry Brown has been a guiding force in the CALM program from its inception in the early 1990s; the influence of his conceptual constructs and their implementation are pervasive in this work.

Disclosure statement

No potential conflict of interest was reported by the author(s).

Funding

This work was supported by U.S. National Science Foundation (NSF) [grant number ARC-1002119, OPP-0352958,OPP-1304555,OPP-1836377,OPP-1836381,OPP-9732051].

ORCID

Kelsey E. Nyland http://orcid.org/0000-0002-9292-4504
Nikolay I. Shiklomanov http://orcid.org/0000-0002-8609-0240
Dmitry A. Streletskiy http://orcid.org/0000-0003-2563-2664
Frederick E. Nelson http://orcid.org/0000-0001-5207-5360
Anna E. Klene http://orcid.org/0000-0002-0579-1628
Alexander L. Kholodov http://orcid.org/0000-0002-7878-8008

References

Abramov, A., Davydov, S., Ivashchenko, A., Karelin, D., Kholodov, A., Kraev, G., Lupachev, A., Maslakov, A., Ostroumov, V., Rivkina, E., Shmelev, D., Sorokovikov, V., Tregubov, O., Veremeeva, A., Zamolodchikov, D., & Zimov, S. (2019). Two decades of active layer thickness monitoring in Northeastern Asia. *Polar Geography*, 1–17. https://doi.org/10.1080/1088937X.2019.1648581

Assmann, J. J., Myers-Smith, I. H., Keryby, J. T., Cunliffe, A. M., & Daskalova, G. N. (2020). Drone data reveal heterogeneity in tundra greenness and phenology not captured by satellites. *Environmental Research Letters*, *15*(12), 125002. https://doi.org/10.1088/1748-9326/abbf7d

Auerbach, N. A., Walker, D. A., & Bockheim, J. (1997). Landcover of the Kuparuk River Basin, Alaska. Tundra Ecosystem Analysis and Mapping Laboratory, University of Colorado, Boulder, 1:250,000. http://www.Colorado.Edu/INSTAAR/TEAML/atlas/

Bhatt, U. S., Walker, D. A., Raynolds, M. K., Bieniek, P. A., Epstein, H. E., Comiso, J. C., Pinzon, J. E., Tucker, C. J., Steele, M., Ermold, W., & Zhang, J. (2017). Changing seasonality of panarctic tundra vegetation in relationship to climatic variables. *Environmental Research Letters*, *12*(5), 055003. https://doi.org/10.1088/1748-9326/aa6b0b

Brown, J., Ferrians, O., Heginbottom, J. A., & Melnikov, E. (2002). Circum-Arctic map of permafrost and ground-ice conditions, Version 2. NSIDC: National Snow and Ice Data Center.

Brown, J., Hinkel, K. M., & Nelson, F. E. (2000). The Circumpolar Active Layer Monitoring (CALM) program: Research designs and initial results. *Polar Geography*, *24*(3), 166–258. https://doi.org/10.1080/10889370009377698

Brown, J., Miller, P. C., Tieszen, L. L., & Bunnell, F. L. (1980). *An Arctic ecosystem: The Coastal Tundra at Barrow, Alaska*. US/IBP Synthesis Series 12, Dowden, Hutchinson and Ross, Inc, 571 pp.

Carter, L. D. (1981). A Pleistocene Sand Sea on the Alaskan Arctic coastal plain. *Science*, *211*(4480), 381–383. https://doi.org/10.1126/science.211.4480.381

Chaudhary, N., Miller, P. A., & Smith, B. (2017). Modelling past, present and future Peatland carbon accumulation across the Pan-Arctic region. *Biogeosciences*, *14*(18), 4023–4044. https://doi.org/10.5194/bg-14-4023-2017

Domine, F., Barrere, M., & Morin, S. (2016). The growth of shrubs on high Arctic tundra at Bylot Island: Impact on snow physical properties and permafrost thermal regime. *Biogeosciences*, *13*(23), 6471–6486. https://doi.org/10.5194/bg-13-6471-2016

Elmendorf, S. C., Henry, G. H., Hollister, R. D., Björk, R. G., Boulanger-Lapointe, N., Cooper, E. J., Cornelissen, J. H. C., Day, T. A., Dorrepaal, E., Elumeeva, T. G., Gill, M., Gould, W. A., Harte, J., Hik, D. S., Hofgaard, A., Johnson, D. R., Johnstone, J. F., Jónsdóttir, I. S., Jorgenson, J. C., … Wipf, S. (2012). Plot-scale evidence of tundra vegetation change and links to recent summer warming. *Nature Climate Change*, *2*(6), 453–457. https://doi.org/10.1038/nclimate1465

Everett, K. R. (1980). Distribution and variability of soils near Atkasook, Alaska. *Arctic and Alpine Research*, *12*(4), 433–446. https://doi.org/10.2307/1550493

Fagan, J. D., & Nelson, F. E. (2017). Spatial sampling design in the Circumpolar Active Layer Monitoring Programme. *Permafrost and Periglacial Processes*, *28*(1), 42–51. https://doi.org/10.1002/ppp.1904

Fisher, R. A., Koven, C. D., Anderegg, W. R. L., Christoffersen, B. O., Dietze, M. C., Farrior, C. E., Holm, J. A., Hurtt, G. C., Knox, R. G., Lawrence, P. J., Lichstein, J. W., Longo, M., Matheny, A. M., Medvigy, D., Muller-Landau, H. C., Powell, T. L., Serbin, S. P., Sato, H., Shuman, J. K., … Moorcroft, P. R. (2018). Vegetation demographics in earth system models: A review of progress and priorities. *Global Change Biology*, *24*(1), 35–54. https://doi.org/10.1111/gcb.13910

Forbes, B. C., Fauria, M. M., & Zetterberg, P. (2010). Russian Arctic warming and 'greening' are closely tracked by tundra shrub willows. *Global Change Biology*, *16*(5), 1542–1554. https://doi.org/10.1111/j.1365-2486.2009.02047.x

Frost, G. V., & Epstein, H. E. (2014). Tall shrub and tree expansion in Siberian tundra ecotones since the 1960s. *Global Change Biology*, *20*(4), 1264–1277. https://doi.org/10.1111/gcb.12406

GCOS. (2003). Second report on the adequacy of the global observing systems for climate in support of the UNFCCC. GCOS Rep. 82, 85 pp. www.wmo.int/pages/prog/gcos/Publications/gcos-82_2AR.pdf

Hinkel, K. M., & Nelson, F. E. (2003). Spatial and temporal patterns of active layer thickness at Circumpolar Active Layer Monitoring (CALM) sites in Northern Alaska, 1995-2000. *Journal of Geophysical Research*, *108*(D2). https://doi.org/10.129/2001JD000927

Hinzman, L. D., Kane, D. L., Gieck, R. E., & Everett, K. R. (1991). Hydrologic and thermal properties of the active layer in the Alaskan Arctic. *Cold Regions Science and Technology*, *19*(2), 95–110. https://doi.org/10.1016/0165-232X(91)90001-W

Hovey, D. (2019, July 16). Fire service says two blazes smoking off of Kougarok road will continue to burn. KNOM Radio Mission. www.knom.org on July 14, 2020

IPCC. (2019). Climate change and land: An IPCC special report on climate change, desertification, land degradation, sustainable land management, food security, and greenhouse gas fluxes in terrestrial ecosystems [P.R. Shukla, J. Skea, E. Calvo Buendia, V. Masson-Delmotte, H.-O. Pörtner, D. C. Roberts, P. Zhai, R. Slade, S. Connors, R. van Diemen, M. Ferrat, E. Haughey, S. Luz, S. Neogi, M. Pathak, J. Petzold, J. Portugal Pereira, P. Vyas, E. Huntley, K. Kissick, M. Belkacemi, J. Malley, (eds.)]. In press.

Kane, D. L., Hinzman, L. D., Benson, C. S., & Everett, K. R. (1991). Hydrology of Imnavait Creek, an Arctic watershed. *Holarctic Ecology*, *12*, 262–269. https://www.jstor.org/stable/3682733

Kane, D. L., & Reeburgh, W. S. (Eds.). (1998). Introduction to special section: Land-Air-Ice Interactions (LAII) flux study. *Journal of Geophysical Research: Atmospheres*, *103*(D22), 28913–28915. https://doi.org/10.1029/1998JD200017

Klene, A. E., Nelson, F. E., Shiklomanov, N. I., & Hinkel, K. M. (2001). The N-factor in natural landscapes: Variability of air and soil-surface temperatures, Kuparuk River Basin, Alaska, U.S.A.. *Arctic, Antarctic, and Alpine Research*, *33*(2), 140–148. https://doi.org/10.1080/15230430.2001.12003416

Koven, C. D., Riley, W. J., & Stern, A. (2013). Analysis of permafrost thermal dynamics and response to climate change in the CMIP5 earth system models. *Journal of Climate*, *26*(6), 1877–1900. https://doi.org/10.1175/JCLI-D-12-00228.1

Krogh, S. A., Pomeroy, J. W., & Marsh, P. (2017). Diagnosis of the hydrology of a small Arctic Basin at the tundra-taiga transition using a physically based hydrological model. *Journal of Hydrology*, *550*, 685–703. https://doi.org/10.1016/j.jhydrol.2017.05.042

Lara, M. J., Nitze, I., Grosse, G., Martin, P., & McGuire, A. D. (2018). Reduced Arctic tundra productivity linked with landform and climate change interactions. *Scientific Reports*, *8*(1), 2345. https://doi.org/10.1038/s41598-018-20692-8

Lawrence, D. M., Oleson, K. W., Flanner, M. G., Fletcher, C. G., Lawrence, P. J., Levis, S., Swenson Sean C., Bonan, G. B. (2012). The CCSM4 land simulation, 1850–2005: Assessment of surface climate and new capabilities. *Journal of Climate*, *25*(7), 2240–2260. https://doi.org/10.1175/JCLI-D-11-00103.1

Lawrence, D. M., & Swenson, S. C. (2011). Permafrost response to increasing Arctic shrub abundance depends on the relative influence of shrubs on local soil cooling versus large-scale climate warming. *Environmental Research Letters*, *6*(4), 045504. https://doi.org/10.1088/1748-9326/6/4/045504

Little, J. D., Sandall, H., Walegur, M. T., & Nelson, F. E. (2003). Application of differential global positioning systems to monitor frost heave and thaw settlement in tundra environments. *Permafrost and Periglacial Processes*, *14*(4), 349–357. https://doi.org/10.1002/ppp.466

Liu, L., Schaefer, K., Zhang, T., & Wahr, J. (2012). Estimating 1992–2000 average active layer thickness on the Alaskan North Slope from remotely sensed surface subsidence. *Journal of Geophysical Research: Earth Surface*, *117*(F1). https://doi.org/10.1029/2011JF002041

Liu, L., Zhang, T., & Wahr, J. (2010). InSAR measurements of surface deformation over permafrost on the North Slope of Alaska. *Journal of Geophysical Research: Earth Surface*, *115*(F3). https://doi.org/10.1029/2009JF001547

Mackay, J. R. (1977). Probing for the Bottom of the Active Layer. *Geological Survey of Canada Paper 77-1A*. pp. 327–328.

McGuire, A. D., Sturm, M., & Chapin, F. S. I. I. I. (2003). Arctic Transitions in the Land–Atmosphere System (ATLAS): Background, objectives, results, and future directions. *Journal of Geophysical Research*, *108*(D2). https://doi.org/10.1029/2002jD002367

Muller, S. V., Walker, D. A., Nelson, F. E., Auerbach, N. A., Bockheim, J., Guyer, S., & Sherba, D. (1998). Accuracy assessment of a land-cover map of the Kuparuk River Basin, Alaska: Considerations for remote regions. *Photogrammetric Engineering and Remote Sensing*, *68*(6), 619–628. https://www.geobotany.uaf.edu/library/pubs/MullerSV1998_pers_64_619.pdf

Myers-Smith, I. H., Forbes, B. C., Wilmking, M., Hallinger, M., Lantz, T., Blok, D., Tape, K. D., Macias-Fauria, M., Sass-Klaassen, U., Lévesque, E., Boudreau, S., Ropars, P., Hermanutz, L., Trant, A., Collier, L. S., Weijers, S., Rozema, J., Rayback, S. A., Schmidt, N. M., … Hik, D. S. (2011). Shrub expansion in tundra ecosystems: Dynamics, impacts and research priorities. *Environmental Research Letters*, *6*(4), 045509. https://doi.org/10.1088/1748-9326/6/4/045509

Nelson, F. E., Hinkel, K. M., Shiklomanov, N. I., Mueller, G. R., Miller, L. L., & Walker, D. A. (1998a). Active-layer thickness in North-Central Alaska: Systematic sampling, scale, and spatial autocorrelation. *Journal of Geophysical Research: Atmospheres*, *103*(D22), 28963–28973. https://doi.org/10.1029/98JD00534

Nelson, F. E., & Outcalt, S. I. (1987). A computational method for prediction and regionalization of permafrost. *Arctic and Alpine Research*, *19*(3), 279–288. https://doi.org/10.2307/1551363

Nelson, F. E., Outcalt, S. I., Brown, J., Hinkel, K. M., & Shiklomanov, N. I. (1998b). Spatial and temporal attributes of the active-layer thickness record, Barrow, Alaska, U.S.A. In A. G. Lewkowicz (Ed.), *Proceedings of the seventh international conference on permafrost* (pp. 797–802). Centre d'études nordiques, Université Laval, Publication No. 57.

Nelson, F. E., Shiklomanov, N. I., Hinkel, K. M., & Brown, J. (2008). Decadal results from the Circumpolar Active Layer Monitoring (CALM) program. In K. M. Hinkel & D. L. Kane (Eds.), *Proceedings of the ninth international conference on permafrost* (pp. 1273–1280). University of Alaska Press.

Nelson, F. E., Shiklomanov, N. I., & Mueller, G. R. (1999). Variability of active-layer thickness at multiple Spatial Scales, North-Central Alaska. U.S.A. *Arctic, Antarctic, and Alpine Research*, *31*(2), 158–165. https://doi.org/10.1080/15230430.1999.12003295

Nelson, F. E., Shiklomanov, N. I., Mueller, G. R., Hinkel, K. M., Walker, D. A., & Bockheim, J. G. (1997). Estimating active-layer thickness over a large region: Kuparuk River Basin, Alaska, U.S.A. *Arctic and Alpine Research*, *29*(4), 367–378. https://doi.org/10.2307/1551985

Ng, E., & Miller, P. C. (1975). Computer simulation of the snowmelt and soil thermal regime at Barrow, Alaska. *Water Resources Research*, *11*(5), 709–715. https://doi.org/10.1029/WR011i005p00709

Nyland, K. E., Nelson, F. E., Streletskiy, D. A., Shiklomanov, N. I., & Brown, J. (2020). Markovian behavior in the response of the permafrost system to climate variability on Alaska's North Slope. *Abstracts, American Geophysical Union Fall Meeting* 2020. (in press).

Nyland, K.E., Shiklomanov, N.I., Streletskiy, D.A., Klene, A.E., Nelson, F.E. (2012). Effect of vegetation on soil-surface temperatures in Northern Alaska. In K. Hinkel (Ed.) *Proceedings of the tenth international conference on permafrost* (Vol. 1, p. 295-300). Salekhard, Russia: The Northern Publisher.

Peel, M. C., Finlayson, B. L., & McMahon, T. A. (2007). Updated world map of the Köppen-Geiger climate classification. *Hydrology and Earth System Sciences*, *11*(5), 1633–1644. https://doi.org/10.5194/hess-11-1633-2007

Raynolds, M. K., & Walker, D. A. (2016). Increased wetness confounds Landsat-Derived NDVI trends in the Central Alaska North Slope Region, 1985–2011. *Environmental Research Letters*, *11*(8), 085004. https://doi.org/10.1088/1748-9326/11/8/085004

Romanovsky, V. E., Smith, S. L., Isaksen, K., Nyland, K. E., Kholodov, A. L., Shiklomanov, N. I., Streletskiy, D. A., Farquharson, L. M., Drozdov, D. S., Makova, G. V., & Christiansen, H. H.

(2020). Terrestrial permafrost [in "State of the Climate in 2018"]. *Bulletin of the American Meteorological Society*, *101*, S265–S271. https://doi.org/10.1175/BAMS-D-21-0086.1

Shiklomanov, N. E., Streletskiy, D. A., & Nelson, F. E. (2012). Northern hemisphere component of the global Circumpolar Active Layer Monitoring (CALM) program. In K. Hinkel (Ed.), *Proceedings of the tenth international conference on permafrost* (Vol. 1, pp. 377–382). The Northern Publisher.

Shiklomanov, N. I. (2001). *Active-layer thickness in the Kuparuk Region, North-Central Alaska: Spatial time series analysis and stochastic modeling* [Ph.D. thesis]. University of Delaware.

Shiklomanov, N. I., & Nelson, F. E. (1999). Analytic representation of the active layer thickness field, Kuparuk River basin, Alaska. *Ecological Modelling*, *123*(2-3), 105–125. https://doi.org/10.1016/S0304-3800(99)00127-1

Shiklomanov, N. I., & Nelson, F. E. (2003). Climate variability in the Kuparuk Region, North-Central Alaska: Optimizing spatial and temporal interpolation in a sparse observation network. *Arctic*, *56* (2), 136–146. https://doi.org/10.14430/arctic609

Shiklomanov, N. I., Nelson, F. E., Streletskiy, D. A., Hinkel, K. M., & Brown, J. (2008, June 29–sJuly 3). The Circumpolar Active Layer Monitoring (CALM) program: Data collection, management, and dissemination strategies. In K. M. Hinkel & D. L. Kane (Eds.), *Proceedings of the ninth international conference on permafrost* (Vol. 2, pp. 1647–1652). Institute of Northern Engineering, University of Alaska Fairbanks.

Shiklomanov, N. I., Streletskiy, D. A., Little, J. D., & Nelson, F. E. (2013). Isotropic thaw subsidence in undisturbed permafrost landscapes. *Geophysical Research Letters*, *40*(24), 6356–6361. https://doi.org/10.1002/2013GL058295

Shur, Y., Hinkel, K. M., & Nelson, F. E. (2005). The transient layer: Implications for geocryology and climate-change science. *Permafrost and Periglacial Processes*, *16*(1), 5–17. https://doi.org/10.1002/ppp.518

Shur, Y. L., & Jorgenson, M. T. (2007). Patterns of permafrost formation and degradation in relation to climate and ecosystems. *Permafrost and Periglacial Processes*, *18*(1), 7–19. https://doi.org/10.1002/ppp.582

Strand, S. M., Christiansen, H. H., Johansson, M., Åkerman, J., & Humlum, O. (2021). Active layer thickening and controls on interannual variability in the Nordic Arctic compared to the circum-Arctic. *Permafrost and Periglacial Processes*, *32*(1), 47–58. https://doi.org/10.1002/ppp.2088

Streletskiy, D. A., Shiklomanov, N. I., Little, J. D., Nelson, F. E., Brown, J., Nyland, K. E., & Klene, A. E. (2017). Thaw subsidence in undisturbed tundra landscapes, Barrow, Alaska, 1962–2015. *Permafrost and Periglacial Processes*, *28*(3), 566–572. https://doi.org/10.1002/ppp.1918

Streletskiy, D. A., Shiklomanov, N. I., Nelson, F. E., & Klene, A. E. (2008, June 29–July 3). Thirteen years of observations at Alaskan CALM sites: Long-term active layer and ground surface temperature trends. In K. M. Hinkel & D. L. Kane (Eds.), *Proceedings of the ninth international conference on permafrost* (Vol. 2, pp. 1727–1732). Institute of Northern Engineering, University of Alaska Fairbanks.

Sturm, M., Racine, C., & Tape, K. (2001). Increasing shrub abundance in the Arctic. *Nature*, *411* (6837), 546–547. https://doi.org/10.1038/35079180

Tape, K. E. N., Sturm, M., & Racine, C. (2006). The evidence for shrub expansion in Northern Alaska and the Pan-Arctic. *Global Change Biology*, *12*(4), 686–702. https://doi.org/10.1111/j.1365-2486.2006.01128.x

Vasiliev, A. A., Drozdov, D. S., Gravis, A. G., Malkova, G. V., Nyland, K. E., & Streletskiy, D. A. (2020). Permafrost degradation in the Western Russian Arctic. *Environmental Research Letters*, *15*(4), 045001. https://doi.org/10.1088/1748-9326/ab6f12

Wahrhaftig, C. (1965). *Physiographic divisions of Alaska*. U.S. Geological Survey Professional Paper, 482, 52 pp.

Walker, D. A., Binnian, E., Evans, B. M., Lederer, N. D., Nordstrand, E., & Webber, P. J. (1989). Terrain, vegetation, and landscape evolution of the R4D research site, Brooks Range Foothills, Alaska. *Holarctic Ecology*, *12*(3), 238–261. https://www.jstor.org/stable/3682732

Walker, D. A., Bockheim, J. G., Chapin, F. S. I. I. I., Eugster, W., King, J. Y., McFadden, J. P., Michaelson, G. J., Nelson, F. E., Oechel, W. C., Ping, C. L., Reeburgh, W. S., Regli, S., Shiklomanov, N. I., & Vourlitis, G. L. (1998). Energy and trace-gas fluxes across a soil pH boundary in the Arctic. *Nature*, *394*(6692), 469–472. https://doi.org/10.1038/28839

Wania, R., Ross, I., & Prentice, I. C. (2009). Integrating peatlands and permafrost into a dynamic global vegetation model: 2. Evaluation and sensitivity of vegetation and carbon cycle processes. *Global Biogeochemical Cycles*, *23*(GB3015), 15. https://doi.org/10.1029/2008GB003412

Weller, G., Chapin, F. S., Everett, K. R., Hobbie, J. E., Kane, D., Oechel, W. C., Ping, C. L., Reeburgh, W. S., Walker, D., & Walsh, J. (1995). The Arctic Flux Study: A regional view of trace gas release. *Journal of Biogeography*, *22*(2/3), 365–374. https://doi.org/10.2307/2845932

Xia, J., McGuire, A. D., Lawrence, D., Burke, E., Chen, G., Chen, X., Delire, C., Koven, C., MacDougall, A., Peng, S., Rinke, A., Saito, K., Zhang, W., Alkama, R., Bohn, T. J., Ciais, P., Decharme, B., Gouttevin, I., Hajima, T., … Luo, Y. (2017). Terrestrial ecosystem model performance in simulating productivity and its vulnerability to climate change in the northern permafrost region. *Journal of Geophysical Research: Biogeosciences*, *122*(2), 430–446. https://doi.org/10.1002/2016JG003384

Zamin, T. J., Bret-Harte, M. S., & Grogan, P. (2014). Evergreen shrubs dominate responses to experimental summer warming and fertilization in Canadian Mesic low Arctic tundra. *Journal of Ecology*, *102*(3), 749–766. https://doi.org/10.1111/1365-2745.12237

Zhang, T., Barry, R. G., Knowles, K., Heginbottom, J. A., & Brown, J. (2008). Statistics and characteristics of permafrost and ground-ice distribution in the Northern Hemisphere. *Polar Geography*, *31*(1-2), 47–68. https://doi.org/10.1080/10889370802175895